

Raman observations of quantum interference in the $\nu_1/2\nu_2$ Fermi dyad region of carbon dioxide

Craig W. McCluskey*

Department of Physics C1600, The University of Texas at Austin, Austin, TX 78712-0264, USA

David S. Stoker

Department of Physics C1600, The University of Texas at Austin, Austin, TX 78712-0264, USA

and

The Center for Nano- and Molecular Science and Technology and the Texas Materials Institute, C2201

The University of Texas at Austin, Austin, TX 78712-1063, USA

(Dated: September 27, 2018)

Coherent anti-Stokes Raman spectra (CARS) were obtained for CO₂ in a positive column discharge. The intensities of the Raman transitions to the $\nu_1/2\nu_2$ Fermi dyad decrease significantly when the discharge is turned on because of equalization of the lower and upper state populations by electron impact excitation, in a manner similar to saturation. The strength of the 1285 cm⁻¹ transition is observed to decrease by a factor of 20 greater than the 1388 cm⁻¹ line due to a quantum interference decreasing the vibrational relaxation rate of the upper state of the 1285 cm⁻¹ transition. This interference is verified by measurements of the decay rates from the state. Experiments ruling out Stark effects and polarization effects are described. Supporting the observed rapid vibrational excitation by electrons, a strong hot band transition $20^0_0 \leftarrow 02^2_0$ at 1425.61 cm⁻¹ was observed. These observations are compared with recent measurements of the Raman spectra of CO₂ heated in a flame.

I. INTRODUCTION

CO₂ has been studied since the earliest days of both infrared and Raman spectroscopy. Rasetti wrote about the Raman effect in gases [1] and selection rules in the Raman effect [2] in 1929. He had noticed, in particular, that the Raman lines observed in CO₂ were quite different than expected, with two lines instead of a single line. Fermi [3] described the origin of these strong Q-branch lines which now bear his name in 1931. Discussions about quantum interference in transitions between the states of CO₂ waited until much later. Zhu *et al.* [4], for example, wrote about quantum interference in the excitation rates in 1991. Quantum interference effects are also observable in relaxation and are the subject of this work.

II. THEORY

A. Anharmonicity in CO₂

The Q-branches in CO₂ at 1285 cm⁻¹ and 1388 cm⁻¹ are the components of the Fermi dyad, a feature due to an “accidental” near degeneracy of one quanta of energy in symmetric stretch, ν_1 , with two quanta of energy in bend, $2\nu_2$ [3]. Because these two frequencies are so close to each other ($\delta = 7.87$ cm⁻¹ [5]) the states $|10^0_0\rangle$ and $|02^0_0\rangle$ strongly perturb each other.

As Herzberg [6] shows, anharmonicities change the total energy of a polyatomic molecule from the sum of $3N$ mutu-

ally independent simple harmonic oscillators of mass 1, to,

$$\mathcal{H} = \frac{1}{2}(\eta_1^2 + \lambda_1\eta_1^2) + \frac{1}{2}(\eta_2^2 + \lambda_2\eta_2^2) + \dots + \sum_{ijk} \alpha_{ijk}\eta_i\eta_j\eta_k + \sum_{ijkl} \beta_{ijkl}\eta_i\eta_j\eta_k\eta_l + \dots \quad (1)$$

where η_i are the normal coordinates of the motions. Thus, the total energy is no longer the sum of independent (even though anharmonic) oscillators.

In CO₂ some of the coefficients α_{ijk} and β_{ijkl} are equal to zero because the potential energy must be unchanged for all symmetry operations of the molecule’s point group, $D_{\infty h}$. Additionally, symmetry operations allow the antisymmetric normal coordinates to occur in Eqn. 1 only in even powers. Of the ten unique cubic terms, then, only α_{111} , α_{122} , and α_{133} are non-zero and the cubic terms of the potential energy are,

$$\alpha_{111}\eta_1^3 + \alpha_{122}\eta_1(\eta_{2a}^2 + \eta_{2b}^2) + \alpha_{133}\eta_1\eta_3^2. \quad (2)$$

α_{122} is the term that generates the anharmonic coupling between ν_1 and $2\nu_2$ that gives the Fermi resonance.

Note that in Raman spectroscopy, the signal is proportional, among other things, to the derivative of the polarizability with respect to position at the equilibrium distance. Because of this, the symmetric stretch normal mode (ν_1) produces a Raman signal, while bend (ν_2) and asymmetric stretch (ν_3) are Raman inactive.

B. Fermi Splitting in CO₂

As Herzberg [6] also shows, in Fermi resonance the two vibrational levels that have nearly the same energy in zero approximation (in CO₂ ν_1 and $2\nu_2$) “repel” each other: one is shifted up and the other is shifted down so that the separation of the two levels is much greater than expected. In addition, a

*Currently with: Los Alamos National Laboratory, N-2, Advanced Nuclear Technology, P.O. Box 1663, M/S B228, Los Alamos, NM 87545 USA; craigm@lanl.gov

mixing of the eigenfunctions of the two states occurs. The deviation of the energy levels from what is expected, as well as the mixing of the eigenfunctions, become greater as the separation of the zero approximation energies becomes smaller.

In addition to depending inversely on the separation of the zero approximation energies, the magnitude of the repulsion depends on the value of the corresponding matrix element W_{ni} of the perturbation function W :

$$W_{ni} = \int \psi_n^0 W \psi_i^{0*} d\tau \quad (3)$$

where W is essentially given by the anharmonic (cubic, quartic, etc.) terms of the potential energy discussed in §II A and ψ_n^0 and ψ_i^0 are the zero approximation eigenfunctions of the two levels. Note that since W has the full symmetry of the molecule, as mentioned above, ψ_n^0 and ψ_i^0 must both have the same symmetry type in order for the integral in (3) to be non-zero. This means that only vibrational levels of the same symmetry can perturb each other. This can be seen in the energy level diagram, Fig. 1, where 10^00 and 02^00 , both being Σ_g^+ , are involved in a Fermi resonance while 02^20 , being Δ_g , is not.

If the separation of the zero approximation energies is fairly small, the magnitude of the shift can be calculated with first-order perturbation theory from the secular determinant,

$$\begin{vmatrix} E_n^0 - E & W_{ni} \\ W_{in} & E_i^0 - E \end{vmatrix} = 0,$$

where, E_n^0 and E_i^0 are the unperturbed energies and $W_{in} = W_{ni}^*$ from Eqn. (3). The perturbed energies are then,

$$E = \bar{E}_{ni} \pm \frac{1}{2} \sqrt{4|W_{ni}|^2 + \delta^2}, \quad (4)$$

where,

$$\begin{aligned} \bar{E}_{ni} &= \frac{1}{2} (E_n^0 + E_i^0) \\ \delta &= (E_n^0 - E_i^0). \end{aligned}$$

The eigenfunctions of the two resulting states are linear combinations of the zero approximation eigenfunctions of the form,

$$\begin{aligned} \psi_n &= a\psi_n^0 - b\psi_i^0 \\ \psi_i &= b\psi_n^0 + a\psi_i^0, \end{aligned} \quad (5)$$

where,

$$\begin{aligned} a &= \left(\frac{\sqrt{4|W_{ni}|^2 + \delta^2} + \delta}{2\sqrt{4|W_{ni}|^2 + \delta^2}} \right)^{\frac{1}{2}}, \\ b &= \left(\frac{\sqrt{4|W_{ni}|^2 + \delta^2} - \delta}{2\sqrt{4|W_{ni}|^2 + \delta^2}} \right)^{\frac{1}{2}}. \end{aligned} \quad (6)$$

Putting Howard-Lock and Stoicheff's values [5],

$$\begin{aligned} W_{10^00-02^00} &= -51.232 \text{ cm}^{-1} \\ \delta &= -7.87 \text{ cm}^{-1}, \end{aligned}$$

in Equations 6 (using the magnitude of δ) gives,

$$a = 0.734, \quad b = 0.679.$$

Identifying ψ_n^0 with $|10^00\rangle$ and ψ_i^0 with $|02^00\rangle$, expressing the coefficients as sines and cosines, and using bracket notation, as do Zhu *et al.* [4], yields,

$$\begin{aligned} |\psi_l\rangle &= \cos\theta |10^00\rangle - \sin\theta |02^00\rangle \\ |\psi_u\rangle &= \sin\theta |10^00\rangle + \cos\theta |02^00\rangle, \end{aligned} \quad (7)$$

with $\theta = 42.8^\circ$ for $^{12}\text{CO}_2$

The magnitude of δ must be used in Equations 6 because if the minus sign from $\delta = -7.87 \text{ cm}^{-1}$ were used, the lower state, $|\psi_l\rangle$, would have an excess $|02^00\rangle$ instead of $|10^00\rangle$, which is the unperturbed state which is actually “repelled” toward it.

C. Notation Conventions

One of the problems in working with CO_2 is the confusion engendered by the profusion of state naming and notation conventions. Adel and Dennison [7] used the notation (v_1, v_2, v_3, ℓ) , where ℓ is the vibrational angular momentum. Herzberg [6] used the notation (v_1, v_2^ℓ, v_3) . Amat and Pimbert [8] used notation similar to Herzberg's but introduced the idea of using 1 and 2 as ranking indices to denote the higher and lower-energy peaks of a Fermi dyad. Schrötter and Brandmüller in Finsterhölzl *et al.* [9] used the notation of Amat and Pimbert, but explicitly labeled states with the ranking index. They, for example, labeled the 1388 cm^{-1} peak as $(10^00)_I$ and the 1285 cm^{-1} peak as $(10^00)_II$. They also labeled the 1410 hotband as $(11^10)_I - (01^10)$ and the 1265 hotband as $(11^10)_II - (01^10)$, keeping for the hotbands some indication of which levels are involved. Rothman and Young used notation similar to that of Schrötter and Brandmüller in their HITRAN (**high resolution transmission**) molecular absorption database intended for atmospheric physicists, but wrote everything out on a single line suitable for a computerized database [10]. In their notation, the 1388 cm^{-1} line is 10001 and the 1285 cm^{-1} line is 10002.

All this confusion is *somewhat* ameliorated by the “Rosetta Stone” of notation in Rothman and Young's 1981 paper on carbon dioxide [11], reproduced below in Table I.

TABLE I: Comparison of notations for CO_2 vibrational energy levels.

Herzberg [6]	Amat [8]	HITRAN [12]
20^00	$(20^00, 04^00)_I$	20001
12^00	$(20^00, 04^00)_{II}$	20002
04^00	$(20^00, 04^00)_{III}$	20003
12^20	$(12^20, 04^20)_I$	12201
04^20	$(12^20, 04^20)_{II}$	12202
04^40	04^40	04401

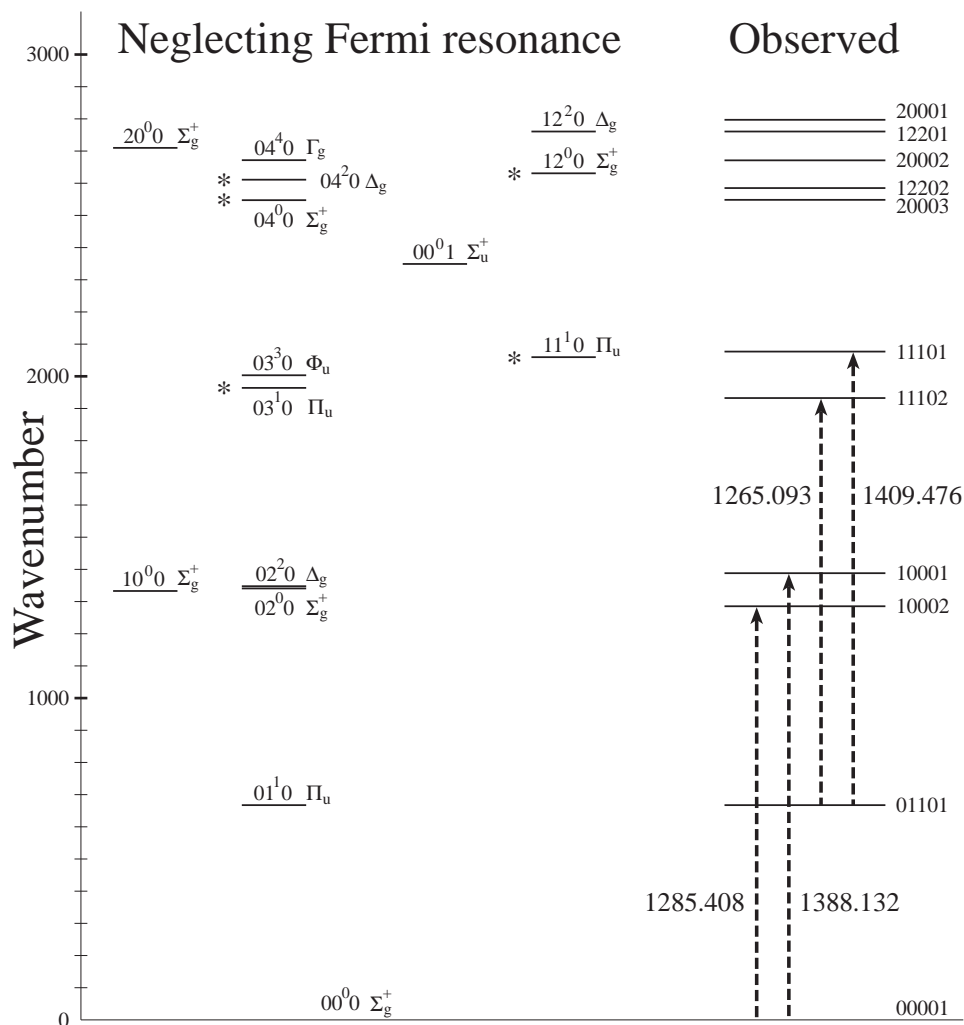


FIG. 1: Energy Levels of CO_2 . Energies of levels marked with an asterisk are uncertain. Strongest Raman transitions are marked by heavy dotted lines.

As one progresses from Herzberg’s notation to the HITRAN notation, it becomes increasingly difficult to know which exact levels are involved and the states involved in the transition become hidden.

The vibrational energy levels of CO_2 are shown in Fig. 1. In this figure, the strongest Raman transitions of CO_2 in the wavenumber range examined are marked by heavy dotted lines. Herzberg’s notation is used on the left to show the locations of where the states would be if they were not perturbed by Fermi resonance. Some of the energy levels of these lines, marked by asterisks, were given in Herzberg [6] but were not given in any of the other references examined. Herzberg’s (old) values of the energies did not make any sense considering Fermi resonance and the (new and more precise) observed levels, which are plotted on the right according to Rothman’s values [13] and marked with HITRAN notation, so the values of these levels were manually adjusted to be more reasonable. Note that in Fig. 1, the non-Fermi resonance influenced levels of 02^2_0 , 03^3_0 , and 04^4_0 are not plotted on the right side for clarity.

III. EXPERIMENTAL APPARATUS AND CONDITIONS

The experimental setup used for this work, described previously in the literature [14], is shown in Fig. 2. The spectrometer consists of a neodymium-YAG laser (using the second harmonic output at $\lambda = 532$ nm), a tunable dye laser pumped by part of the output of the YAG laser, optics to overlap both spatially and temporally the remainder of the YAG laser’s output (which is represented by the box labeled “Pump Laser” in Fig. 2) with the output of the dye laser inside the sample volume, and optics to detect the newly created CARS beam coming from the sample cell. A quartz block in a squeezing mechanism is used as a variable wave-plate (VWP) to adjust the polarization of the incident YAG beam. Fig. 2 also shows optics and electronics for detection of Raman induced Kerr-effect signals, which were used previously [14]. For this experiment, the “pick-off” prism (P2 in Fig. 2), the double monochromator, and the photomultiplier tube (PMT) were added to detect the coherent anti-Stokes Raman spectroscopy (CARS) signal.

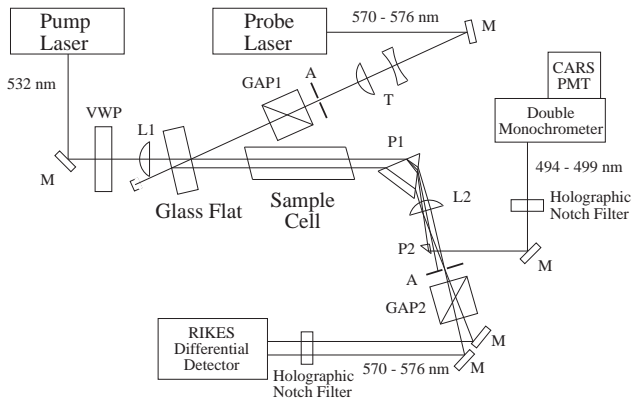


FIG. 2: Spectrometer Optics Layout. A: aperture, GAP: Glan-air polarizer, L: lens, M: mirror, P: prism, T: Galilean telescope, VWP: Variable wave plate.

The Pyrex glass linear discharge cell used for the majority of the experiments is shown in Fig. 3. It consists of two concentric glass tubes and has both a hollow cathode and a hollow anode. The inner glass tube is 1'' O.D. at the ends and

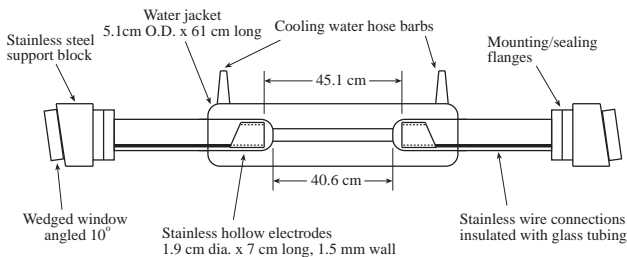


FIG. 3: The Linear Discharge Cell.

necks down to an inner diameter of 0.375'' over its central 16 inches. The smaller cross-section confines the glow discharge and yields a higher current density. The ends of the inner glass tube are open for mounting to stainless steel support blocks at each end. The outer glass tube forms a water-cooling jacket which cools not only the region of the discharge, but also beyond the electrodes.

When running, the cell provides a long positive column glow discharge which extends four to five inches on both sides of the focus of the YAG and dye laser beams so the region probed by the most intense portions of the focused laser beams is within the positive column. At a current of 100 mA, the current density is 1400 A/m² (0.14 A/cm²).

IV. RESULTS

As can be seen in Fig. 4 and 5, both peaks of the Fermi dyad drop when the discharge is turned on. Surprisingly, the 1285 cm⁻¹ line drops much more than the 1388 cm⁻¹ line. This was true over broad ranges of both pressures and discharge currents.

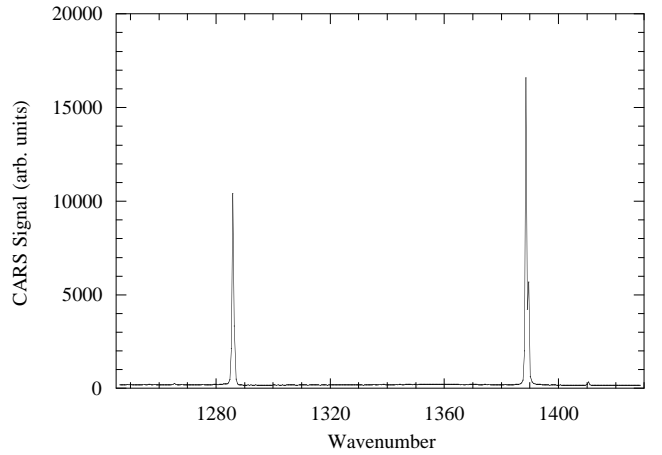


FIG. 4: Spectrum of carbon dioxide with discharge off.

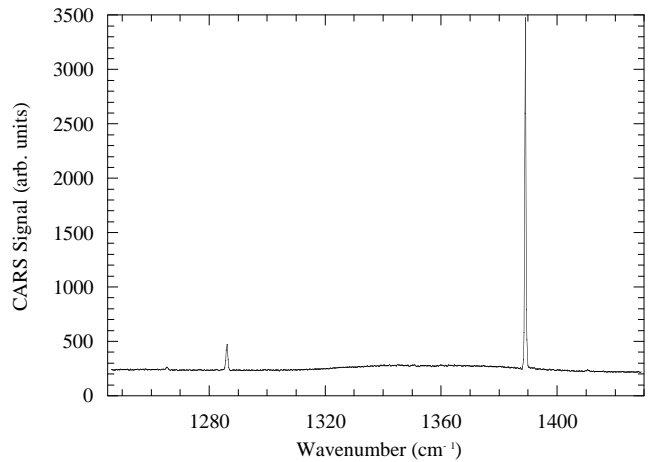


FIG. 5: Spectrum of carbon dioxide with discharge on.

A. Drop of Both Fermi Dyad Peaks

The drop of *both* peaks when the discharge is turned on is expected because the gas in the discharge is hotter and less dense than the gas with no discharge. It is also vibrationally heated, leading to the depletion of the ground state. In their report of spontaneous Raman investigations of the pure rotational lines in CO₂ Barrett *et al.* [15] stated the intensity of the lines with their discharge on (run at 10 mA and a pressure of 40 Torr) was about $\frac{1}{5}$ the intensity with the discharge off. They calculated the temperature of their discharge (from the strongest pure rotational line) to be 730 K.

In this experiment, such a measurement is not possible. The temperature can be estimated, however, by calculating the relative signal strength of the 1285 cm⁻¹ and 1388 cm⁻¹ peaks to the 1265 cm⁻¹ and 1410 cm⁻¹ hotband peaks as a function of temperature and then matching the ratio with what is observed.

The population of a specific state is given by,

$$N_i = N \frac{g_i e^{-\frac{E_i}{kT}}}{Q_v(T)}, \quad (8)$$

where, N is the total number of atoms, N_i , g_i , and E_i are the population, degeneracy factor, and the energy of the i^{th} state and $Q_v(T)$ is the vibrational partition function.

The CARS signal is proportional to the square of the difference between two states, $(\Delta N_{12})^2$, so the ratio of the intensity of the ground state peaks to that of the hotband peaks is given by,

$$\left(\frac{N_0 - N_2}{N_1 - N_3}\right)^2 = \left(\frac{g_0 - g_2 e^{-\frac{E_2}{kT}}}{g_1 e^{-\frac{E_1}{kT}} - g_3 e^{-\frac{E_3}{kT}}}\right)^2. \quad (9)$$

Fig. 6 shows the detail of the baseline of the discharge-on spectrum. The large hump in the middle of the spectrum is background noise which remains when the cell is evacuated and which may be a Raman signal from the optics.

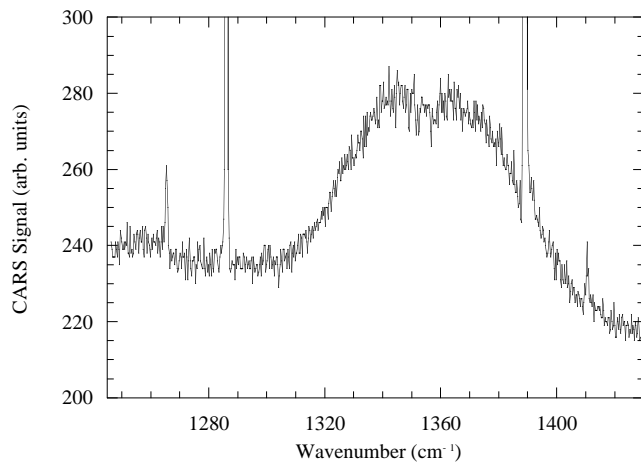


FIG. 6: Baseline of spectrum of Fig. 5 showing hotbands.

The ratio of the summed areas of the 1285 cm^{-1} and 1388 cm^{-1} ground state peaks (7393) to the summed areas of the 1265 cm^{-1} and 1410 cm^{-1} hotband peaks (172) is 42.983. (Note that the baseline was manually placed for each peak to compensate for the dispersive parts of the lineshapes.) Solving Eqn. 9 iteratively for T gives a discharge-on temperature of 373 K (quite a bit lower than Barrett's 730 K). Note that this analysis assumes that the mechanisms exciting a molecule from the ground state to one of the hotbands are in thermal equilibrium with the mechanisms de-exciting from the hotband to the ground state. As will be shown in §IV C, this is an invalid assumption.

Nevertheless, this increased temperature would be expected to reduce the density and cause a drop of signal strength by a factor of 1.60 but there is an additional contribution from depletion of the ground state by vibrational heating. To calculate this contribution, it is necessary to use Eqns. 8 and 9 to calculate the exact ground state and excited state populations for the discharge-off and discharge-on temperatures of 295 K and 373 K. Since the exponentials in Q_v rapidly become very small only a limited number of terms are needed. This analysis uses the states shown in Fig. 1, all of which are below 3000 cm^{-1} . The calculation shows the ground state population decreasing from 92% of the molecules with the discharge

off to 67% of the molecules with the discharge on and 25% of the molecules being shifted from the ground state to higher states. Including the density factor with the vibrational heating, the 1285 cm^{-1} and 1388 cm^{-1} peaks should drop by a factor of 1.9.

Since the 1285 cm^{-1} and 1388 cm^{-1} peaks decrease by more than a factor of 19, much more than Barrett's factor of 5, there is an additional source of decrease in $(\Delta N_{12})^2$.

One of the possibilities is that the ground state is being depopulated because the CO_2 is being converted to other molecules. Barrett, for example, considered that the drop in signal might be due to the CO_2 molecules being converted to CO_2^+ . He estimated the concentration of these ions in the discharge to be about $3 \times 10^{11} \text{ ions/cm}^3$, an insignificant concentration compared to his gas density of $10^{18}/\text{cm}^3$. Mass spectrometric measurements of discharges have found other ions, such as O_2^+ , but the total concentrations were low [16, 17, 18, 19, 20]. This would also rule out large concentrations of dissociation products.

B. Greater Drop of 1285 cm^{-1} Peak

In considering the greater drop of the 1285 cm^{-1} peak (10002) than the 1388 cm^{-1} peak (10001), it must be kept in mind that the magnitude of the CARS signal depends upon the square of the difference in population of the upper and lower states. To have one peak drop more than the other, then, the ratio of the differences in populations must be affected. This suggests four possibilities:

- The transition rate is altered or the degeneracy of the harmonic states broken,
- Raman saturation of upper levels,
- The discharge saturates the final state of the 1285 cm^{-1} transition, or,
- The discharge changes the relaxation rates from the unperturbed states.

Since both 10001 and 10002 begin in the ground state, it is possible that the transition rate to 10002 is altered or the near-degeneracy of the states 10^0 and 02^0 is changed. Such, however, would require a shift of the wavenumber of the peaks and none was observed (within a resolution of 0.2 cm^{-1}) when the discharge was turned on. No change in the ratio of intensities of 10001 and 10002 was also observed when the electric field was applied without a discharge.

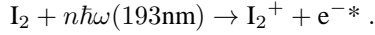
If the molecule is illuminated by strong enough laser beams, the transition could be saturated with equal populations in the upper and lower states. To test this, the YAG laser intensity was varied by an order of magnitude. No significant change in the ratio of intensities of 10001 and 10002 was observed.

The third possibility is not as easily addressed as the first two. If the discharge saturates the population of 10002, its intensity will be decreased relative to 10001. This would require

an electron excitation rate of $|\psi_l\rangle$ in Eqn. 7 greater than that of $|\psi_u\rangle$. Zhu *et al.* [4], however, observed exactly the opposite.

Their experimental setup was completely different than the one used in this work and they worked at a much lower pressure (27.5 milli Torr).

They produced translationally hot electrons, e^{-*} , by multi-photon ionization of iodine with an ArF laser at 193 nm:



These translationally hot electrons then collided with CO_2 molecules causing rotational and vibrational excitation of the 10001 and 10002 states. By tuning their diode laser, operating at ($\lambda \approx 4.3\mu\text{m}$), they could probe specific rotational lines of the CO_2 molecules by absorption in the strongly allowed ν_3 (anti-symmetric stretch) infrared band using the transitions $10^00 \rightarrow 10^01$ and $02^00 \rightarrow 02^01$. They concluded that the upper state, $|\psi_u\rangle$ is significantly more populated by electron scattering than the lower state, $|\psi_l\rangle$, by a factor of 9.1 to 12.7, depending on the particular J state examined.

Looking at the collisional excitation probability from the ground state to the upper excited state, P_{gu} , and to the lower excited state P_{gl} ,

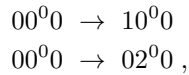
$$P_{gu} \propto |\sin\theta \langle 10^00 | V | 00^00 \rangle + \cos\theta \langle 02^00 | V | 00^00 \rangle|^2$$

$$P_{gl} \propto |\cos\theta \langle 10^00 | V | 00^00 \rangle - \sin\theta \langle 02^00 | V | 00^00 \rangle|^2$$

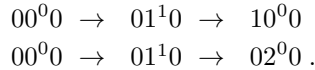
where V defines the interaction potential. If one assumes the electron excitations $\langle 10^00 | V | 00^00 \rangle$ and $\langle 02^00 | V | 00^00 \rangle$ are nearly equal, Zhu's results follow from these probabilities. The minus sign in the equation for $|\psi_l\rangle$ then causes a ‘‘quantum interference’’ in its electron excitation rate, causing the upper state of $|\psi_l\rangle$ to have a lower population than the upper state of $|\psi_u\rangle$. This is in contrast to the present observations where $|\psi_l\rangle$'s weaker signal implies a higher population in its upper state. Since one would expect that a change in population that affects the infrared signal in one way would not affect the CARS signal in another, there must be a difference in the experiments to cause different results.

The difference is that Zhu *et al.* used ‘‘hot’’ electrons, a significant fraction of which had energies around 3 eV, while our experiment produces mean electron energies on the order of 0.1 eV. Their higher energy electrons opened up an excitation channel that was unavailable to the lower energy electrons of this experiment.

Counting as separate the unperturbed states making up $|\psi_l\rangle$ and $|\psi_u\rangle$, there are four paths of excitation from the ground state to $|\psi_l\rangle$ and $|\psi_u\rangle$. As shown in Fig. 7, there are two direct paths marked with the circled ‘‘1’’,



and two indirect paths marked with the circled ‘‘2’’,



The single quantum, direct excitation of 10^00 from 00^00 occurs most readily in the discharge. Mazevet *et al.* [21] showed

that the vibrationally inelastic excitation cross-section for $e\text{-CO}_2$ scattering peaks around 0.2 eV, quite close to the average electron energy in the discharge of 0.1 eV mentioned in the previous section.

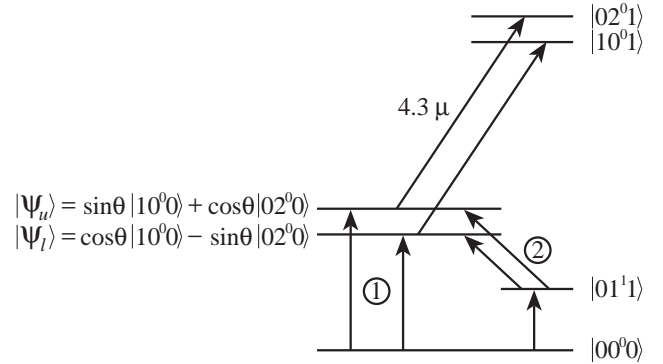


FIG. 7: CO_2 excitation paths.

The double quantum, direct excitation of 02^00 from 00^00 is through the intermediate state of CO_2^- . CO_2^- , which can have a lifetime as long as 90 μs in the gas phase [22], has a bond angle of 134.9° [23], so the bend vibration is strongly excited through the decay of CO_2^- . The potential energy curves of CO_2^- are, however, roughly 3 eV higher than those of CO_2 [24, 25], so this excitation channel was open to Zhu *et al.* but closed in the present experiment.

Both indirect paths go through the singly excited bend state 01^10 as an intermediate. Its excitation energy of 667 cm^{-1} (0.083 eV) is matched to the average electron energy in the discharge. The second half of the first indirect path, $00^00 \rightarrow 01^10 \rightarrow 10^00$, is a two quantum transition — it requires a change of v_1 from zero to one and a simultaneous change of v_2 from one to zero — whose probability is therefore low. The second half of the second indirect path, $00^00 \rightarrow 01^10 \rightarrow 02^00$, is a single quantum transition and requires nearly the same energy as the first half of the indirect paths. It thus has a high probability and is the route for excitation of 02^00 in this experiment.

The difference between the results seen by Zhu *et al.*'s experiment and the present one is that Zhu *et al.* had direct excitations from the ground state, 00^00 , to the final state, $|\psi_l\rangle$ or $|\psi_u\rangle$, through two coherent channels, one exciting 10^00 and the other exciting 02^00 . Because these two channels can occur coherently during a single electron excitation process, they saw interference between them and thus a lower excitation probability for the production of $|\psi_l\rangle$. The present experiment, using ‘‘cool’’ electrons, in contrast, has direct excitation $00^00 \rightarrow 10^00$, but indirect, two-step excitation $00^00 \rightarrow 01^10 \rightarrow 02^00$. Since these two processes are incoherent there is no interference and the excitation probabilities of $|\psi_l\rangle$ and $|\psi_u\rangle$ are similar, leading to the conclusion that the discharge could not have preferentially saturated one of the observed states.

The fourth and remaining possibility for explaining this result is that the discharge changes the relaxation rates from the unperturbed states. Here the minus sign of $|\psi_l\rangle$ in Eqn. 7 does

explain what was seen. If turning on the discharge causes the transition rates for the unperturbed states, 10^00 and 02^00 , to become more equal, the quantum interference engendered by the minus sign in Eqn. 7 will cause $|\psi_l\rangle$ to have a much smaller relaxation rate to the lower levels, 01^10 and 00^00 , than $|\psi_u\rangle$. (It can readily be seen that the relaxation rates can be different between discharge on and discharge off because when the discharge is off, relaxation occurs by spontaneous emission and inelastic collisions with molecules and the walls (collision induced emission). When the discharge is turned on, relaxation additionally occurs by inelastic and superelastic collisions with free electrons and ion and electron charge (\vec{E} field) induced emission.)

The significant drop of the 1285 cm^{-1} peak can thus be explained by the discharge causing changes in the relaxation rates from the unperturbed states and saturating the state $|\psi_l\rangle$. Note that the majority of observed drop of the 1388 cm^{-1} line could also be due to the state $|\psi_u\rangle$ being partially saturated by the discharge.

To test this hypothesis, the change of 1285 cm^{-1} and 1388 cm^{-1} CARS signals as a function of time after the discharge was turned off was measured for pressures between 0.8 to 4 Torr. These data are graphed in Fig. 8 and 9.

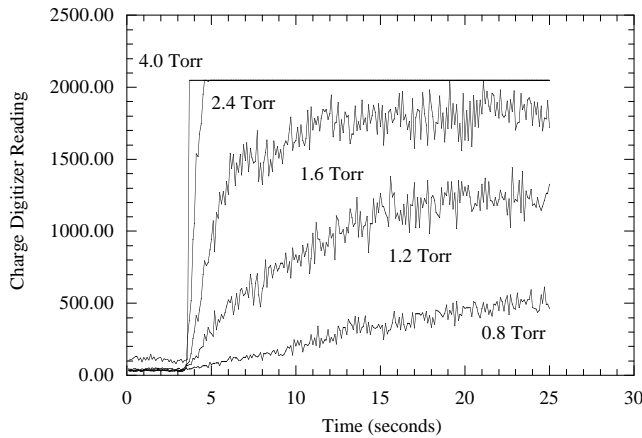


FIG. 8: Rise of 1285 cm^{-1} signal of CO_2 with turn-off of discharge.

For a pressure of 1.6 Torr, for example, the 1388 cm^{-1} signal increased as an exponential with a time constant $\tau \approx 2.0 \pm 0.3\text{ s}$. The increase in signal is due to both the decrease of population in $|\psi_u\rangle$ and the repopulation of the ground state from other levels by collisions. This vibrational relaxation time for repopulating the ground state decreases with increasing pressure as expected.

Under the same conditions, the growth of the 1285 cm^{-1} signal due to $|\psi_l\rangle$ exhibits a double-exponential behavior whose shorter time constant is consistent with the repopulation of the ground state. These data are re-plotted in Fig. 10 with the curve fit. The results of this analysis are consistent with the model of quantum interference altering the vibrational relaxation rate from $|\psi_l\rangle$ compared with that from $|\psi_u\rangle$.

Others have measured relaxation rates from CO_2 states but their results are not applicable to this experiment.

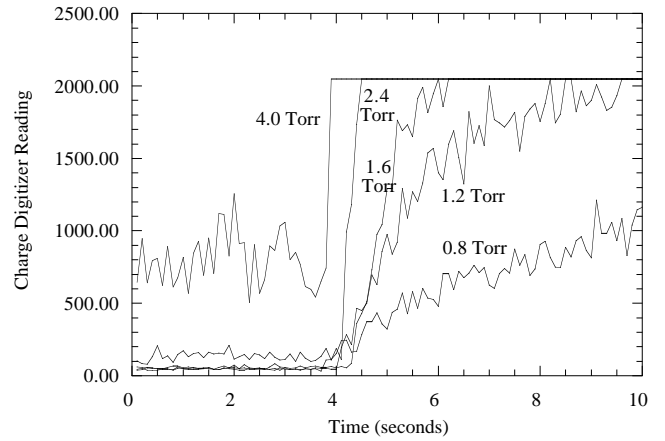


FIG. 9: Rise of 1388 cm^{-1} signal of CO_2 with turn-off of discharge.

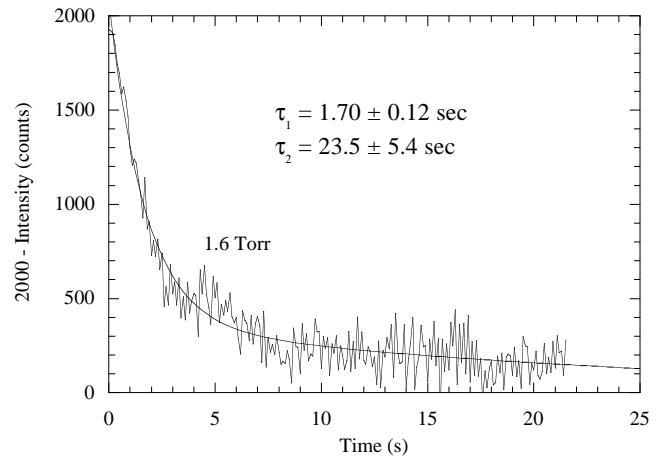


FIG. 10: Rise of 1285 cm^{-1} signal of CO_2 at 1.6 Torr with double exponential fit.

Roche *et al.* [26], for example, measured relaxation of the $\nu_1/2\nu_2$ Fermi dyad with Raman-infrared double resonance using a CO_2 laser to continuously monitor populations via the 9.4 or $10.4\ \mu\text{m}$ CO_2 laser transitions much in the same way as Zhu *et al.* used their diode laser. Instead of exciting CO_2 molecules with hot electrons or H(D) atoms, they selectively excited the molecules with a doubled-YAG/dye laser setup similar to the one used in the present work — though theirs achieved narrow-band dye operation with an argon laser pumped CW dye oscillator. They measured the vibrational relaxation rate versus pressure from the 1388 cm^{-1} peak. Since the 1388 cm^{-1} peak is very narrow the rotational lines blend at low pressures (0.006 amagat, 5 Torr). Because of this, they excited all of the rotational lines, which lead to achieving rotational equilibrium more rapidly and making the vibrational relaxation more efficient. They were able to resolve the 1285 cm^{-1} Q-branch and used that to measure the rotational relaxation rate versus pressure from that state. Unfortunately, they do not give the vibrational relaxation rate from the 1285 cm^{-1} peak and do not give any results for CO_2 in a discharge. Dang *et al.* [27] measured

the relaxation times of CO_2 vibrational levels in a discharge. They disturbed the discharge-on equilibrium with a CO_2 laser pulse and then watched as that equilibrium was re-established with the discharge remaining on. In this experiment, in contrast, the discharge-on relaxation rates are compared with the discharge-off relaxation rates and a change in the rates when the discharge is turned on is what causes the 1285 cm^{-1} peak to drop more than the 1388 cm^{-1} peak.

C. Visibility of Saturation of $|\psi_l\rangle$ in Spectra

If, as posited in the previous section, the 1285 cm^{-1} signal drops more than the 1388 cm^{-1} signal because its lower relaxation rate causes a saturation of the upper level of the transition, that saturated upper level should then be the lower level of hotband transitions that appear when the discharge is turned on. The possible transitions out of both the 1285 cm^{-1} and 1388 cm^{-1} states with energies similar to those of the present investigation are shown in Table II. Of the ten candidates,

TABLE II: Hotband transitions out of 1285 cm^{-1} and 1388 cm^{-1} states.

Upper State		Lower State	
		10001 (1388.18 cm^{-1})	10002 (1285.41 cm^{-1})
20003	(2548.37 cm^{-1})	1160.18	1262.96
12202	(2585.02 cm^{-1})	1196.84	1299.61
20002	(2671.14 cm^{-1})	1282.96	1385.73
12201	(2760.72 cm^{-1})	1372.54	1475.32
20001	(2797.14 cm^{-1})	1408.95	1511.73

six are within the 1245 cm^{-1} to 1430 cm^{-1} range examined experimentally. Of these six, the three from 1285 cm^{-1} should be stronger than the three from 1388 cm^{-1} . In addition, two of the transitions ($12201 \leftarrow 10001$ at 1372.54 cm^{-1} and $12202 \leftarrow 10002$ at 1299.61 cm^{-1}) involve the change of only the number of quanta of the bend vibration, ν_2 . As mentioned in §II A, the ν_2 vibration is Raman inactive and so, absent any concomitant change in the symmetric stretch (ν_1) quantum number or Fermi mixing, should not be visible at all.

The baselines of many discharge-on spectra were examined for evidence of lines at these wavenumbers. Of the six candidates, 1299.61 cm^{-1} , 1385.73 cm^{-1} , and 1408.95 cm^{-1} suggest the possibilities of lines.

The spectrum examined previously for computation of the temperature of the discharge (Fig. 6) is reproduced in Fig. 11 with an arrow pointing at the possible line at 1299.61 cm^{-1} , heavily influenced by noise. Its weakness is not surprising in view of the Raman inactivity of the transition.

Fig. 12 shows the region of the 1388 cm^{-1} Q-branch with the solid arrow pointing at the possible line at 1385.73 cm^{-1} . The weakness of this line is surprising given the degree of saturation expected for the upper state of the 1285 cm^{-1} Q-branch, $|\psi_l\rangle$, though it could be explained by a small Raman

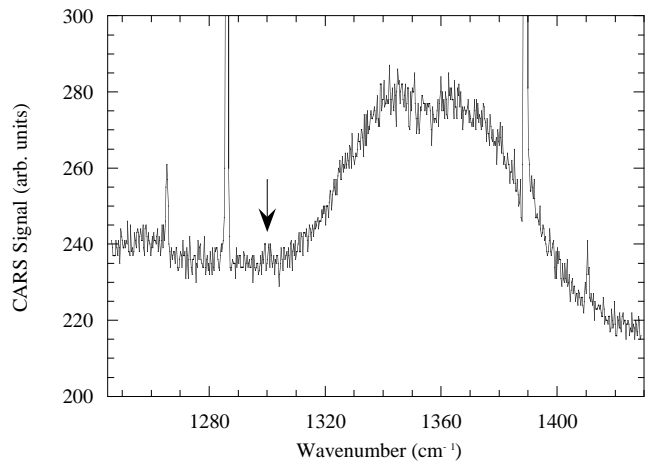


FIG. 11: Baseline of CO_2 spectrum showing 1299.61 cm^{-1} line when discharge is turned on.

cross-section for the transition. It is also possible that the that

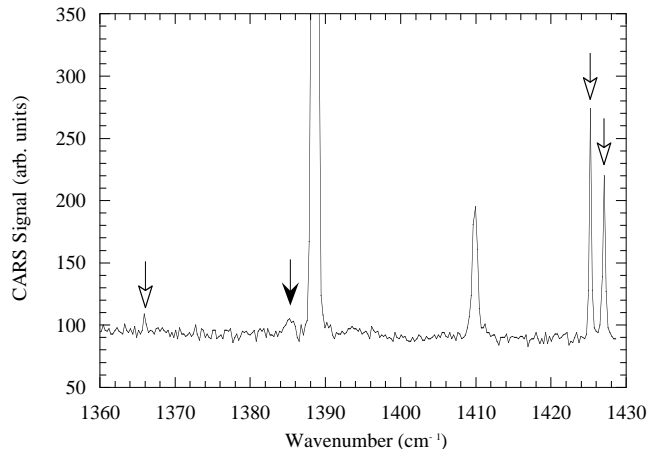


FIG. 12: Baseline of CO_2 spectrum showing 1385.73 cm^{-1} line (solid arrow) and additional lines at 1366 , 1424 , and 1426 cm^{-1} when the discharge is turned on (hollow arrows).

the cross-products between a line and its neighbors and between a line and the background inherent in the $|\chi^{(3)}|^2$ probed by CARS destructively interfere and reduce the strength of the line.

Fig. 13 shows a comparison of the no discharge and 100 mA discharge spectra of $11101 \leftarrow 01101$ hotband at 1409.476 cm^{-1} . Note that the discharge on peak is broader and is less symmetric than the discharge off peak, being shaded to the lower energy side, where the $20001 \leftarrow 10001$ hotband would be. In contrast to the amplitude of the 1385 cm^{-1} line just discussed, here there is no question that the cross-products in the $|\chi^{(3)}|^2$ change the shape and placement of the lines. This effect could be avoided by using RIKES instead of CARS. Since this line arises from the upper state of the 1388 cm^{-1} Q-branch, $|\psi_u\rangle$, its weakness is expected.

Interestingly, however, it was noticed that when the dis-

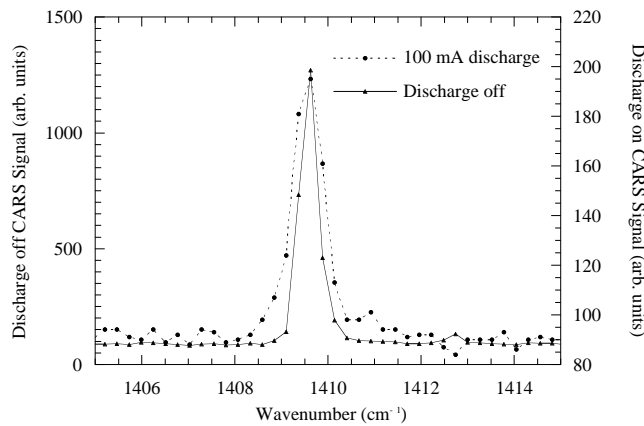


FIG. 13: Baseline of CO₂ spectra showing comparison of 1409.476 cm⁻¹ hotband with discharge off (solid line) and on (dotted line).

charge was on, there were repeatable, clearly resolvable lines at 1366, 1424, and 1426 cm⁻¹. These lines are marked in Fig. 12 with hollow arrows. From Rothman's data [13], the 1366 cm⁻¹ line is due to the transition 10011 ← 00011, the 1424 cm⁻¹ line to 21101 ← 11101, and the 1426 cm⁻¹ line to 12201 ← 02201, where 02201 is the two quanta bend vibrational state with two quanta of vibrational angular momentum that is not involved in Fermi resonance with 10001. Though hotband transitions directly from the saturated 10001 and 10002 states are not observed, the strong hotband from 02201 only 50 cm⁻¹ away suggests large populations of all three levels. This validates the saturation model.

Note that in Fig. 12, the amplitude of the line at 1424 cm⁻¹ (which originates from the 02201 state at 1335.15 cm⁻¹) is greater than that of the line at 1410 cm⁻¹ (which originates from the 01101 state at 667.3799 cm⁻¹), whereas a Boltzman distribution at 373 K would require the opposite. This indicates that the gas temperature calculated in §IV A from the ratio of the populations is incorrect, that the vibrational energy of the molecules is not in thermal equilibrium with the temperature of the gas but is more on the order of the temperature of the electrons, which for energies of 0.1 – 0.2 eV is roughly 1000 – 2000 K. This is not surprising because the molecules are excited to upper levels by electron impact while they are de-excited back to the ground state by collisions with other molecules. In fact, with separate processes, one would be surprised if the excitation and de-excitation rates were equal and

thermal equilibrium were achieved.

In contrast to the very selective population of upper levels by electron impact evident in low pressure spectra, spectra taken at higher pressures show a much more thermal distribution. In Fig. 14, the intensities of the excited state lines show a monotonic decrease in strength, exactly what one would expect from a Boltzman distribution and similar to what has been shown previously for work in flames [28] and in furnaces [29]; the quantum interference in the 1285 and 1388 cm⁻¹ lines is still apparent.

Quantum interference is present in other transitions of CO₂ as well. Table II shows that a line at 1511 cm⁻¹ due to the transition 20001 ← 10002 should be observed. Since this transition is due to an increase of the Raman-active symmetric stretch quantum number, one would expect it to be quite visible. Experimentally, however, this line is not seen, even in spectra at 40 Torr. In this case, the level 20001 is composed of the states 20⁰⁰ + 12⁰⁰ + 04⁰⁰ and the level 10002 is composed of the states 10⁰⁰ – 02⁰⁰. Here excitation by the path 12⁰⁰ ← 02⁰⁰ (with the minus sign) interferes with excitation by the path 20⁰⁰ ← 10⁰⁰ and the total excitation probability vanishes. It is also interesting to note that the 1409 cm⁻¹ hotband, perhaps seen only as a broadening in Fig. 13, is more distinct as a separate peak in Fig. 14.

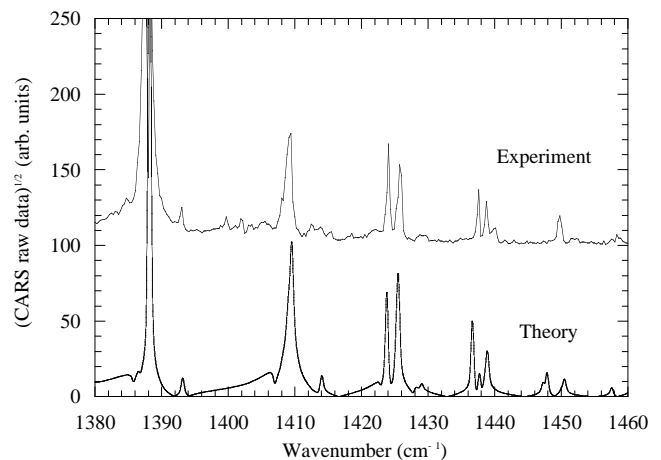


FIG. 14: High pressure CO₂ spectra showing higher-order hotbands. Note that the 1388 cm⁻¹ peak in the experimental (upper) trace is saturated; the strong signals at 40 Torr overload the electronics.

[1] F. Rasetti, *Nature* **123**, 205 (1929).
 [2] F. Rasetti, *Nature* **123**, 757 (1929).
 [3] E. Fermi, *Zeitschrift für Physik* **71**, 250 (1931).
 [4] L. Zhu, S. A. Hewitt, and G. W. Flynn, *The Journal of Chemical Physics* **94**, 4088 (1991).
 [5] H. E. Howard-Lock and B. P. Stoicheff, *Journal of Molecular Spectroscopy* **37**, 321 (1971).
 [6] G. Herzberg, *Molecular Spectra and Molecular Structure*, vol. II. Infrared and Raman Spectra of Polyatomic Molecules (D.

Van Nostrand Company, Inc., 1945).
 [7] A. Adel and D. M. Dennison, *Physical Review* **43**, 716 (1933).
 [8] G. Amat and M. Pimbert, *Journal of Molecular Spectroscopy* **16**, 278 (1965).
 [9] H. Finsterhölzl, H. W. Klöckner, K. Srinivasan, H. W. Schrötter, and J. Brandmüller, *Indian Journal of Pure & Applied Physics* **16**, 370 (1978).
 [10] L. Rothman, ed., *The HITRAN Database* (Harvard-Smithsonian Center for Astrophysics, World Wide Web,

- <http://www.hitran.com>, 2002).
- [11] L. S. Rothman and L. D. G. Young, *Journal of Quantitative Spectroscopy and Radiative Transfer* **25**, 505 (1981).
- [12] R. A. McClatchey, W. S. Benedict, S. A. Clough, D. E. Burch, R. F. Calfee, K. Fox, L. S. Rothman, and J. S. Garing, Tech. Rep., Air Force Geophysics Laboratory, Hanscom AFB, MA 01731 (1973).
- [13] L. S. Rothman, R. L. Hawkins, R. B. Wattson, and R. R. Gamache, *Journal of Quantitative Spectroscopy and Radiative Transfer* **48**, 537 (1992).
- [14] P. S. Bhatia, J. P. Holder, and J. W. Keto, *Journal of the Optical Society of America B* **14**, 263 (1997).
- [15] J. J. Barrett and A. Weber, *Journal of the Optical Society of America* **60**, 70 (1970).
- [16] J. M. Austin and A. L. S. Smith, *Journal of Physics D: Applied Physics* **5**, 468 (1972).
- [17] M. Saporoschenko, *Physical Review A (General Physics)* **8**, 1044 (1973).
- [18] J. A. J. III and R. Ramaiah, *Physical Review A (General Physics)* **36**, 774 (1987).
- [19] S. V. K. Kumar and V. S. Venkatasubramanian, *The Journal of Chemical Physics* **79**, 6423 (1983).
- [20] J. A. Rees and S. R. Alger, *Proceedings of the Institution of Electrical Engineers* **126**, 356 (1979).
- [21] S. Mazevet, M. A. Morrison, L. A. Morgan, and R. K. Nesbet, *Physical Review A* **64**, 040701 (2001).
- [22] R. N. Compton, P. W. Reinhardt, and C. D. Cooper, *The Journal of Chemical Physics* **63**, 3821 (1975).
- [23] A. R. Rossi and K. D. Jordan, *The Journal of Chemical Physics* **70**, 4422 (1979).
- [24] D. Spence and G. J. Schulz, *The Journal of Chemical Physics* **60**, 216 (1974).
- [25] C. R. Claydon, G. A. Segal, and H. S. Taylor, *The Journal of Chemical Physics* **52**, 3387 (1970).
- [26] C. Roche, G. Millot, R. Chauv, and R. Saint-Loup, *The Journal of Chemical Physics* **101**, 2863 (1994).
- [27] C. Dang, J. Reid, and B. K. Garside, *Applied Physics B* **31**, 163 (1983).
- [28] R. J. Blint and J. H. Bechtel, *Journal of Quantitative Spectroscopy and Radiative Transfer* **23**, 89 (1980).
- [29] R. L. Farrow, P. E. Schrader, T. A. Reichardt, and R. J. Gallagher, in *2000 Glass Industry Project Review, Oak Ridge, Tennessee* (Combustion Research Facility, Sandia National Laboratories, Livermore, CA 94550, 2000).